arXiv:1408.3529v1 [cond-mat.str-el] 15 Aug 2014

Effective models for the magnetization behavior of Shastry-Sutherland model

Brijesh Kumar* and Bimla Danu
School of Physical Sciences, Jawaharlal Nehru University, New Delhi 110067, India
(Dated: August 18, 2014)

The minimal effective model for the magnetisation plateaus below 1/2 in the Shastry-Sutherland model is derived to be an Ising model of certain unit-cell hard-core bosons with anisotropic repulsive interactions on isosceles triangular lattice. It unambiguously gives the prominent plateaus at 1/8, 1/6, 1/4, 1/3 and an additional one at 3/8, related through a particle-hole (p-h) transformation. The Dzyaloshinsky-Moriya (DM) interaction dresses it up with an inhomogeneous transverse field that also causes p-h asymmetry due to an in-plane component of the inter-dimer DM vector. This explains the asymmetry between the magnetisation below and above 1/4 in $SrCu_2(BO_3)_2$. The effective model above 1/2 plateau is an XXZ model with stronger XY parts. It gives no magnetisation plateaus, but exhibits chiral order.

PACS numbers: 75.10.Jm, 75.10.Hk, 75.60.Ej, 05.30.Jp

The Shastry-Sutherland (SS) model, and the material $SrCu_2(BO_3)_2$ that realises it, are subjects of great current interest [1, 2]. This compound is a layered spin-gapped Mott insulator in which the Cu^{2+} dimers in $CuBO_3$ layers form the frustrated SS lattice of antiferromagnetically coupled quantum spin-1/2's [3, 4]. The most notable feature of $SrCu_2(BO_3)_2$ is the occurrence of plateaus in the magnetisation, M, as a function of the magnetic field, h, at certain fractional values of the saturation magnetisation, M_{sat} [2, 5]. This phenomenon has drawn much attention, and inspired a lot of studies.

Experimentally, the most prominent plateaus occur at $M/M_{sat} = 1/8$, 1/4 and 1/3. The other plateaus at 1/9, 1/7, 1/6, 1/5 and 2/9 have also been reported through torque measurements [6]. The plateau at 1/6 has been confirmed recently, and an additional one at 2/15 has been reported [7]. Above 1/3, the plateaus at 2/5 and 1/2 have also been reported [8]. While the plateau at 1/2 has been confirmed, the one at 2/5 seems absent, in recent ultra-high field measurements upto 118T [9]. Except 1/8, 1/6, 1/4, 1/3 and 1/2, there appears to be a lack of consensus on the more exotic fractions.

These discoveries have led to a great deal of research on the Shastry-Sutherland model, $\hat{H}_{SS}$, which is the basic quantum spin-1/2 model for $SrCu_2(BO_3)_2$ [10].

$$\hat{H}_{SS} = J \sum_{\langle i,j \rangle} \mathbf{S}_i \cdot \mathbf{S}_j + J' \sum_{\langle l,m \rangle} \mathbf{S}_l \cdot \mathbf{S}_m - h \sum_i S_i^z \quad (1)$$

Here, J is the intra-dimer exchange and J' is the inter-dimer coupling, both antiferromagnetic (see Fig. 1). For $SrCu_2(BO_3)_2$, various estimates give $J'/J \approx 0.63$ [9, 10], which implies that its low temperature spin-gapped phase is a direct-product of the singlets on Cu^{2+} dimers (the exact ground state of $\hat{H}_{SS}$) [11]. The Dzyaloshinsky-Moriya (DM) interaction is also present as a small perturbation to the leading picture set by the SS model [12–14].

The early studies on $\hat{H}_{SS}$ found the dimer-triplet excitations to be highly localised objects [3]. Thus, for $h \neq 0$, the magnetisation behaviour of the SS model, and that of the $SrCu_2(BO_3)_2$, is understood to be dominated by the interactions between the field-induced triplets (effective hard-core bosons), competed at best by the correlated hopping processes [10, 15]. Accordingly, the crystalline superstructures of the localised triplets, stabilised by interactions, characterise the magnetisation plateaus, as observed at 1/8 through NMR [16]. Away from a plateau, but near its ends, there could also arise a supersolid phase, wherein M grows smoothly, while the crystalline order of triplets has not melted [15, 17]. These ideas have advanced to sophisticated levels of computation through the pCUT (perturbative continuous unitary transformations) [18] and CORE (contractor-renormalization) methods [19]. An alternate approach is the Chern-Simons (CS) theory [20], which has predicted a series of plateaus at $1/q$ for $9 \geq q \geq 2$ and 2/9 [6].

While the effective models in terms of the dimer-hard-core bosons [21] have been generated to very high orders in J'/J, and they do give a host of plateaus, but they look obscure and don't offer much clarity into whether a plateau occurs and why. In this Letter, we try to change this situation by deriving a simple effective model for the magnetisation behaviour of the SS model. Through this, we unambiguously get all the prominent plateaus at 1/8, 1/6, 1/4, 1/3 and 1/2, and an additional one at 3/8. We also understand that the plateaus at 1/8 and 3/8 occur as a pair, and the same for 1/6 and 1/3, related via the particle-hole transformation in the minimal model, and how DM interaction affects this feature. Our effective model for $M/M_{sat} \leq 1/2$, in its barest form, is a classical problem (Ising model) of hard-core bosons with repulsive interactions on isosceles triangular lattice, which is dressed by the transverse-field like quantum fluctuations due to DM interaction. We also derive a minimal effective model for $M/M_{sat} \geq 1/2$, which is an XXZ problem on isosceles triangular lattice. It gives no plateaus (except some anomalies near 1/2 and 1), but a chiral order.

The basic premise of our study is a doubt whether the dimer-hard-core bosons can ever lead to a neat and

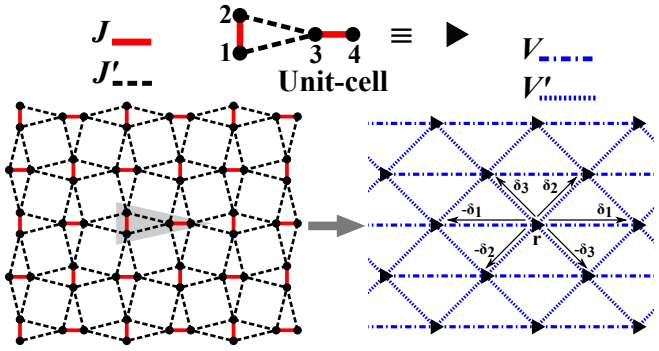

FIG. 1. The Shastry-Sutherland model Eq. (1), and the corresponding isosceles triangular lattice model Eq. (2).

decisive understanding of the magnetisation behaviour of the SS model [22]. It is because the orthogonal-dimer topology of the SS lattice renders the J' links around a dimer-singlet ineffective by annihilation, which makes it hard to reconstruct the dynamics in terms of the dimer-hard-core bosons. It comes as no surprise, therefore, that the corresponding effective models remain obscure, and despite the progress, leave one in doubt about the finality of their outcome.

We overcome this difficulty by working with the eigenstates of $J(\mathbf{S}_1\cdot\mathbf{S}_2+\mathbf{S}_3\cdot\mathbf{S}_4)+J'(\mathbf{S}_1+\mathbf{S}_2)\cdot\mathbf{S}_3$, a natural 'crystallographic' unit-cell of the SS lattice (see Fig. 1). These states carry in them at least some effect of the J' exactly, which for the dimer-states would require much extra effort to reconstruct. These eigenstates are presented in Table I, and their eigenvalues are plotted as a function of J'/J, and h, in Fig. 2. For a basic effective description of the SS model in magnetic field, it would suffice to work with $|0\rangle\equiv|0,0;ss\rangle$ and $|1\rangle\equiv|1,1;-\rangle$ for $M/M_s\leq\frac{1}{2}$, and $|1\rangle$ and $|2\rangle\equiv|2,2\rangle$ for $M/M_{sat}\geq\frac{1}{2}$.

For $M/M_{sat}\leq 1/2$, we derive the effective Hamiltonian, $\hat{H}_{\leq\frac{1}{2}}=E_{(0;ss)}L+\hat{H}_0+\hat{H}_X+\hat{H}_{DM}$, by reorganising the SS lattice in terms of these unit-cells without breaking the translational symmetry, and projecting each unit-cell onto its $\{|0\rangle,|1\rangle\}$ basis. Here, $E_{(0;ss)}L$ is the singlet energy of L unit-cells. The $\hat{H}_0$ is the *minimal* effective Hamiltonian for the SS model, in terms of the "cell-hard-core bosons" (defined in Table II), on the isosceles triangular lattice of Fig. 1, with total L sites.

$$\hat{H}_0=\sum_{\mathbf{r}}\hat{n}_{\mathbf{r}}\left[-\tilde{h}+V\hat{n}_{\mathbf{r}+\delta_1}+V'\left(\hat{n}_{\mathbf{r}+\delta_2}+\hat{n}_{\mathbf{r}+\delta_3}\right)\right] \quad (2)$$

The effective interactions, $V=J'(3+\cos\theta)(1-\cos\theta+2\sqrt{2}\sin\theta)/32$ and $V'=J'(3+\cos\theta)(1-\cos\theta)/32$, are repulsive, and V is always stronger than V' (see Fig. 3). The 'chemical potential', $\tilde{h}=h-\Delta_1$, controls the filling of these hard-core particles with energy-gap $\Delta_1=E_{(1;-)}-E_{(0;ss)}$.

The $\hat{H}_X$ denotes the corrections beyond $\hat{H}_0$. One could generate it, say, by using the pCUT method with our unit-cell states. But here we do something very simple. We add some more repulsion, just a little beyond V and V'. That is, we consider $\hat{H}_X=\sum_{\mathbf{r}}\hat{n}_{\mathbf{r}}[V''\hat{n}_{\mathbf{r}+\delta_2+\delta_3}+V'''(\hat{n}_{\mathbf{r}+\delta_1+\delta_2}+\hat{n}_{\mathbf{r}-\delta_1+\delta_3})]$. This is not quite ad hoc. We know these interactions would be there, and expect $V'''\lesssim V''$ to be very small [23]. Heuristically, we estimate $V''\sim\frac{V}{32}(\sin\theta)^4$, and take $V'''\approx V''$ for the calculations below.

Now we discuss M/M_{sat} vs. h using $\hat{H}_0+\hat{H}_X$. Here, $M=\sum_{\mathbf{r}}\langle\hat{n}_{\mathbf{r}}\rangle$ and $M_{sat}=2L$. While h likes to populate the lattice with hard-core bosons (cell-triplets), the repulsive interactions like them to stay as far away from

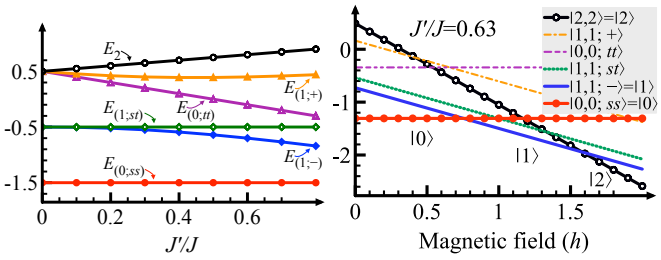

FIG. 2. Eigenvalues of a single unit-cell of the Shastry-Sutherland model plotted as a function of J'/J, and h.

TABLE I. The eigenstates of a single unit-cell of the Shastry-Sutherland model (see Fig. 1), in terms of the singlet, $|s\rangle$, and the triplets, $|t_m\rangle$ for $m=1,0,\bar{1}$, on the bonds (1,2) and (3,4).[a]

Eigenstates [b]	Eigenvalues
Singlets	
$\|0,0;ss\rangle=\|s\rangle_{12}\|s\rangle_{34}$	$E_{(0;ss)}=-3J/2$
$\|0,0;tt\rangle=\frac{\|t_1\rangle_{12}\|t_{\bar{1}}\rangle_{34}-\|t_0\rangle_{12}\|t_0\rangle_{34}+\|t_{\bar{1}}\rangle_{12}\|t_1\rangle_{34}}{\sqrt{3}}$	$E_{(0;tt)}=\frac{J}{2}-J'$
Triplets[c]	
$\|1,m;st\rangle=\|s\rangle_{12}\|t_m\rangle_{34}$	$E_{(1;st)}=-J/2$
$\|1,m;\pm\rangle=\cos(\theta_\pm/2)\|1,m;tt\rangle+\sin(\theta_\pm/2)\|1,m;ts\rangle$	$E_{(1;\pm)}=-\frac{J'}{4}\pm\sqrt{\left(\frac{J}{2}-\frac{J'}{4}\right)^2+\frac{J'^2}{2}}$
Quintets [d]	
$\|2,2\rangle=\|t_1\rangle_{12}\|t_1\rangle_{34}$	$E_2=(J+J')/2$
$\|2,1\rangle=\frac{\|t_1\rangle_{12}\|t_0\rangle_{34}+\|t_0\rangle_{12}\|t_1\rangle_{34}}{\sqrt{2}}$	
$\|2,0\rangle=\frac{\|t_1\rangle_{12}\|t_{\bar{1}}\rangle_{34}+2\|t_0\rangle_{12}\|t_0\rangle_{34}+\|t_0\rangle_{12}\|t_1\rangle_{34}}{\sqrt{6}}$	

[a] The bond-states on (1,2) are: $|s\rangle_{12}=\frac{|\uparrow_1\downarrow_2\rangle-|\downarrow_1\uparrow_2\rangle}{\sqrt{2}}$, $|t_1\rangle_{12}=|\uparrow_1\uparrow_2\rangle$, $|t_0\rangle_{12}=\frac{|\uparrow_1\downarrow_2\rangle+|\downarrow_1\uparrow_2\rangle}{\sqrt{2}}$ and $|t_{\bar{1}}\rangle_{12}=|\downarrow_1\downarrow_2\rangle$, and likewise on bond (3,4). The negative m's are denoted as $\bar{m}$.

[b] The eigenstates are denoted as $|S_{uc},m_{uc};\text{extra-labels}\rangle$, where S_{uc} is the total spin quantum-number of the unit-cell, m_{uc} is the corresponding z-component, and the 'extra-labels' indicate (when necessary) the spins of the bond-states [on (1,2) and (3,4), respectively] that make it.

[c] Here, the triplet states $|1,m;ts\rangle=|t_m\rangle_{12}|s\rangle_{34}$, and $|1,m;tt\rangle$ are given as: $|1,1;tt\rangle=\{|t_1\rangle_{12}|t_0\rangle_{34}-|t_0\rangle_{12}|t_1\rangle_{34}\}/\sqrt{2}$, $|1,0;tt\rangle=\{|t_1\rangle_{12}|t_{\bar{1}}\rangle_{34}-|t_{\bar{1}}\rangle_{12}|t_1\rangle_{34}\}/\sqrt{2}$, and $|1,\bar{1};tt\rangle=\{|t_0\rangle_{12}|t_{\bar{1}}\rangle_{34}-|t_{\bar{1}}\rangle_{12}|t_0\rangle_{34}\}/\sqrt{2}$. Moreover, $\theta_\pm=\theta+\pi\frac{1\mp1}{2}$, where $\tan\theta=2\sqrt{2}J'/(2J-J')$.

[d] The states $|2,\bar{2}\rangle$ and $|2,\bar{1}\rangle$ can be obtained from $|2,2\rangle$ and $|2,1\rangle$, respectively, by replacing $|t_1\rangle$ with $|t_{\bar{1}}\rangle$.

TABLE II. Representation of the spins in a unit-cell in the basis, $\{|0\rangle, |1\rangle\}$, where $|0\rangle = |0, 0; ss\rangle$ and $|1\rangle = |1, 1; -\rangle$.[a]

$S_{1x} = -S_{2x} = \frac{\cos(\theta/2)}{2\sqrt{2}}\tau^x$	$S_{3x} = S_{4x} = S_{3y} = S_{4y} = 0$
$S_{1y} = -S_{2y} = -\frac{\cos(\theta/2)}{2\sqrt{2}}\tau^y$	$S_{3z} = \frac{(1-\cos\theta-2\sqrt{2}\sin\theta)}{8}\hat{n}$
$S_{1z} = S_{2z} = \frac{(3+\cos\theta)}{8}\hat{n}$	$S_{4z} = \frac{(1-\cos\theta+2\sqrt{2}\sin\theta)}{8}\hat{n}$

[a] Here, $\hat{n} = |1\rangle\langle 1| \equiv (\hat{\mathbf{1}} + \tau^z)/2$, $\hat{\mathbf{1}} = |0\rangle\langle 0| + |1\rangle\langle 1|$ is the identity, $\tau^+ = |1\rangle\langle 0| \equiv \hat{b}^\dagger$, $\tau^x = \tau^+ + \tau^-$ and $\tau^y = -i(\tau^+ - \tau^-)$.

each other as possible. The first plateau would thus correspond to a filling that barely avoids repulsion. For $\hat{H}_0$, it is $M/M_{sat} = 1/6$ with a rhombic superlattice of hard-core particles (a honeycomb of 'holes') shown in Fig. 4. But a non-zero V'' or V''', *howsoever small*, immediately realises 1/8 as the lowest plateau with a square superlattice of cell-triplets (Kagomé lattice of holes) by pushing 1/6 higher up in energy. The lower ($c1$) and upper ($c2$) critical fields for these plateaus (at $T = 0K$) are: $\tilde{h}_{c1}^{(\frac{1}{8})} = 0$ and $\tilde{h}_{c2}^{(\frac{1}{8})} = \tilde{h}_{c1}^{(\frac{1}{6})} = 4(V''+2V''')$. The smallness of V'' and V''' is qualitatively consistent with the small experimental width (~ 1 T) of 1/8 plateau.

To deduce the higher M plateaus, we use the particle-hole (p-h) transformation, $\hat{n}_{\mathbf{r}} \to \hat{\mathbf{1}} - \hat{n}_{\mathbf{r}}$, under which $M/M_{sat} \to \frac{1}{2} - M/M_{sat}$, $\tilde{h} \to 2(V+2V'+V''+2V''') - \tilde{h}$, while V, V', V'' and V''' remain the same. Clearly, it implies a plateau at 3/8 due to the one at 1/8. Likewise, it gives a plateau at 1/3 due to 1/6. Since $\hat{H}_0 + \hat{H}_X$ is invariant under p-h transformation for $\tilde{h} = V+2V'+V''+2V'''$ at $M/M_{sat} = 1/4$, it naturally brings in the plateau at 1/4. Besides, the 1/2 is trivially there. The superlattice structures at 1/3 and 3/8 plateaus are obtained by p-h transforming ($0 \leftrightarrow 1$) the structures at 1/6 and 1/8, respectively. At 1/4, the cell-triplets form stripes, as in Fig. 4, consistent with what is known. The critical fields obtained by comparing the energies of these ordered states are: $\tilde{h}_{c2}^{(\frac{1}{6})} = \tilde{h}_{c1}^{(\frac{1}{4})} = 3V' - 2V'' - V'''$, and $\tilde{h}_{c2}^{(\frac{1}{4})} = \tilde{h}_{c1}^{(\frac{1}{3})}$, $\tilde{h}_{c2}^{(\frac{1}{3})} = \tilde{h}_{c1}^{\frac{3}{8}}$ and $\tilde{h}_{c2}^{(\frac{3}{8})} = \tilde{h}_{c1}^{(\frac{1}{2})}$ can be determined from the p-h transformation rule for $\tilde{h}$. Thus, all the prominent plateaus (1/8, 1/6, 1/4, 1/3 and 1/2) arise naturally and unambiguously in our very simple effective model, $\hat{H}_0 + \hat{H}_X$. It also gives an additional plateau at

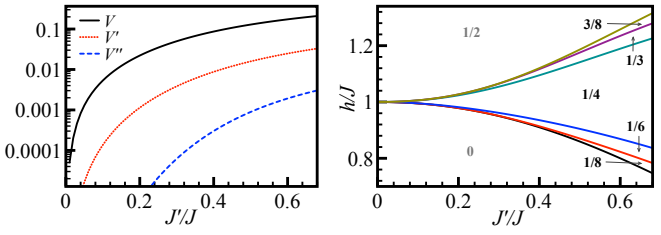

FIG. 3. The interactions (left), and the plateau phase diagram (right), within $\hat{H}_0 + \hat{H}_X$ for $0 \le M/M_{sat} \le 1/2$.

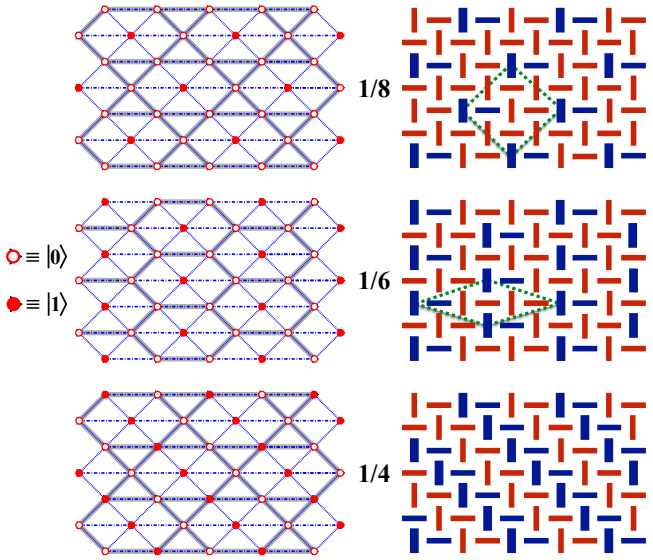

FIG. 4. The cell-triplet superlattices at $M/M_{sat} = 1/8$, 1/6 and 1/4 plateaus within $\hat{H}_0 + \hat{H}_X$, and the corresponding dimer-triplet orders on SS lattice. Here, the blue bonds with two different thicknesses denote dimer-triplets with different weights, and the red ones are the dimer-singlets. The ordered structures at 1/3 and 3/8 can be obtained by particle-hole transformation, $|0\rangle \leftrightarrow |1\rangle$, on 1/6 and 1/8 states, respectively.

3/8. These we have also checked by exact energy minimisation (on small clusters) and monte carlo simulations of this effective model [24]. Next we discuss the effects of DM interaction, relevant to $SrCu_2(BO_3)_2$, on $\hat{H}_0 + \hat{H}_X$.

At low temperatures, the intra-dimer DM vector in $SrCu_2(BO_3)_2$ lies in the plane of dimers and $\perp$ to the dimer's orientation, and the inter-dimer DM interaction is kind of arbitrary [14]. By projecting them onto the local $\{|0\rangle, |1\rangle\}$ basis, we get the following effective $\hat{H}_{DM}$.

$$\hat{H}_{DM} = \sum_{\mathbf{r}} \left[\hat{\mathcal{D}}^x_{\mathbf{r}}(-\delta_2, \delta_3)\tau^x_{\mathbf{r}} + \hat{\mathcal{D}}^y_{\mathbf{r}}(-\delta_1, -\delta_2, \delta_3)\tau^y_{\mathbf{r}} \right] \quad (3)$$

Here, $\hat{\mathcal{D}}^x_{\mathbf{r}}(-\delta_2, \delta_3) = D'_y(\sin\theta\cos\frac{\theta}{2})(\hat{n}_{\mathbf{r}+\delta_3} - \hat{n}_{\mathbf{r}-\delta_2})/4$ and $\hat{\mathcal{D}}^y_{\mathbf{r}}(-\delta_1, -\delta_2, \delta_3) = -\frac{D}{2\sqrt{2}}\cos\frac{\theta}{2} + \frac{D'_x}{8\sqrt{2}}(\sin\theta\sin\frac{\theta}{2})[\hat{n}_{\mathbf{r}+\delta_3} + \hat{n}_{\mathbf{r}-\delta_2} - 2(\frac{V}{V'})\hat{n}_{\mathbf{r}-\delta_1}]$ are the effective 'transverse fields' dependent upon the local occupancies, $\hat{n}_{\mathbf{r}}$'s. The intra-dimer DM interaction is denoted as D ($\sim 0.03J$), $D'_{x,y}$ ($\lesssim D$) are the x and y components of the inter-dimer DM vector, and $V/V' = 1 + 2\sqrt{2}\cot\frac{\theta}{2}$. Thus, the minimal effective model for the magnetisation behaviour of $SrCu_2(BO_3)_2$, $\hat{H}_0 + \hat{H}_X + \hat{H}_{DM} = \hat{H}_{\le\frac{1}{2}}$, is a 'quantum Ising' model with 'dynamically' inhomogeneous transverse fields [25]. Under the p-h transformation, $D'_x \to -D'_x$, $D'_y \to D'_y$ and $D \to D + \frac{D'_x}{\sqrt{2}}\sin\theta$. An important physical implication of these rules is that a non-zero D'_x [amplified by V/V' (~ 7 for $J'/J = 0.63$)] causes p-h *asymmetry* between the related plateaus, which is indeed there in $SrCu_2(BO_3)_2$. For instance, the plateaus

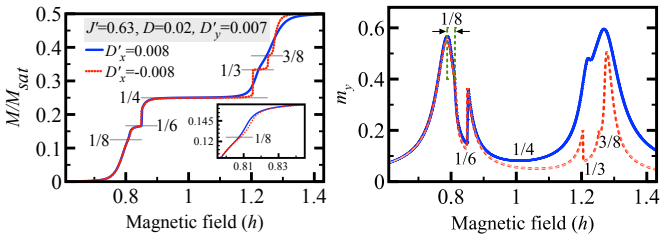

FIG. 5. (Left) M vs. h in the ground state of $\hat{H}_{\leq\frac{1}{2}}$. Notice the asymmetry below and above 1/4, pronounced differently for different signs of D'_x. (Inset) Enlarged view of magnetisation around 1/8. (Right) The transverse magnetisation, $m_y = \frac{1}{L}\sum_{\mathbf{r}}\langle\tau^y\rangle$, for the same values of parameters (with $J=1$).

at 1/6 and 1/3 differ in widths, and 3/8 is still not seen, while 1/8 is too well known. Such p-h asymmetry can also arise due to the three-body interactions in $\hat{H}_X$, but here, we have discussed only the most essential physical content of the $SrCu_2(BO_3)_2$, viz. SS model, problem below 1/2. The results of an exact numerical computation in the ground state of $\hat{H}_{\leq\frac{1}{2}}$ on a 12-sites periodic cluster are shown in Fig. 5. The m_y there gives the staggered transverse magnetisation on (vertical) dimers. The jumps between successive plateaus (and in m_y) is due to the change in the underlying crystalline order (see Fig. 4). Clearly, the $\hat{H}_{\leq\frac{1}{2}}$ is in broad qualitative agreement with the experiments, and can be improved quantitatively by pCUTs, CORE or any other suitable methods.

Interestingly, the recently suggested devil's staircase in $SrCu_2(BO_3)_2$ [7] is a *possibility* within our model, as it is known to occur in the frustrated Ising models with anisotropic interactions [26], which is what $\hat{H}_0+\hat{H}_X$ is, albeit with weak competing interactions ($V'\sim V/10$ and $V''\sim V/100$ as per our estimates in Fig. 3). It would be nice to see if the improved theoretical values of these effective interactions help in the occurrence of devil's staircase. One may also consider estimating these effective parameters 'phenomenologically'.

We also like to remark that the 'superfluidity' and 'supersolidity' are misnomers in the context of $SrCu_2(BO_3)_2$ due to the absence of continuous symmetry in $\hat{H}_{\leq\frac{1}{2}}$, a quantum Ising model. The magnetisation (longitudinal or transverse) in this system does not arise by spontaneously breaking a continuous symmetry.

Overall, this highly simple effective model presents a confident and insightful picture of the magnetisation behaviour of the SS model and $SrCu_2(BO_3)_2$, as compared to the vastly complex dimer-hard-core boson models. Our choice of the unit-cell states, it appears, is the right way to formulate and study this problem.

Finally, encouraged by the discussion below 1/2, we similarly derive a minimal effective Hamiltonian above the 1/2 plateau in terms of the hard-core bosons defined in the $\{|1\rangle,|2\rangle\}$ basis (see Table III). It can be written as: $\hat{H}_{\geq\frac{1}{2}} = -\mu\sum_{\mathbf{r}}\hat{n}_{\mathbf{r}}+\sum_{\mathbf{r}}[U\hat{n}_{\mathbf{r}}\hat{n}_{\mathbf{r}+\delta_1}+t(\hat{b}^\dagger_{\mathbf{r}}\hat{b}_{\mathbf{r}+\delta_1}+h.c)]+\sum_{\mathbf{r}}\sum_{\delta=\delta_2,\delta_3}[U'\hat{n}_{\mathbf{r}}\hat{n}_{\mathbf{r}+\delta}+t'(\hat{b}^\dagger_{\mathbf{r}}\hat{b}_{\mathbf{r}+\delta}+h.c)]+e_0L$. The various model parameters are: $U=J'(1-\cos\theta)(3+\cos\theta-2\sqrt{2}\sin\theta)/32$, $U'=V'$, $t=J'(\sqrt{2}\sin\theta+\cos\theta-1)/8$, $t'=-J'(1-\cos\theta)/8$, $\mu=(h-\Delta_2)+2U+4U'+\frac{J'}{2\sqrt{2}}(\sin\theta-3\sqrt{2})$, and $e_0=E_{(1;-)}+U+2U'+\frac{J'}{2\sqrt{2}}\sin\theta$. For $J'/J\in[0,1]$, t, U and U' all are positive, and $t'<0$. Moreover, $0\approx U\ll U'\lesssim|t'|<t<0.09$. It is an XXZ model on isosceles triangular lattice, with a dominant XY part. Here, we again calculate the magnetisation, $M/M_{sat}=(1+\frac{1}{L}\sum_{\mathbf{r}}\langle\hat{n}_{\mathbf{r}}\rangle)/2$, as a function of h. Due to the weak U and U', and strong quantum fluctuations, we don't expect any crystalline order of triplets, and thus, no plateaus. We did exact numerical diagonalization (ED) on periodic clusters of L upto 21, and a 12-sublattice cluster mean-field theory (CMFT) on a 12-sites exact cluster coupled to the mean-fields at the boundary. Both these calculations give smooth M vs. h curves (see Fig. 6).

TABLE III. Representation of the spins in a unit-cell in the basis, $\{|1\rangle,|2\rangle\}$, where $|1\rangle=|1,1;-\rangle$ and $|2\rangle=|2,2\rangle$.[a]

$S^x_1=S^x_2=\frac{1}{4}\sin\frac{\theta}{2}\tau^x$	$S^x_3=-p_\theta\tau^x$	$S^x_4=q_\theta\tau^x$
$S^y_1=S^y_2=-\frac{1}{4}\sin\frac{\theta}{2}\tau^y$	$S^y_3=p_\theta\tau^y$	$S^y_4=-q_\theta\tau^y$
$S^z_1=S^z_2=\frac{3+\cos\theta}{8}(\hat{\mathbf{1}}-\hat{n})+\frac{1}{2}\hat{n}$	$S^z_3=\tilde{p}_\theta(\hat{\mathbf{1}}-\hat{n})+\frac{1}{2}\hat{n}$	$S^z_4=\tilde{q}_\theta(\hat{\mathbf{1}}-\hat{n})+\frac{1}{2}\hat{n}$

[a] Here, $p_\theta=\frac{1}{2}(\frac{1}{\sqrt{2}}\cos\frac{\theta}{2}+\frac{1}{2}\sin\frac{\theta}{2})$, $q_\theta=\frac{1}{2}(\frac{1}{\sqrt{2}}\cos\frac{\theta}{2}-\frac{1}{2}\sin\frac{\theta}{2})$, $\tilde{p}_\theta=\frac{1}{8}(1-\cos\theta-2\sqrt{2}\sin\theta)$, and $\tilde{q}_\theta=\frac{1}{8}(1-\cos\theta+2\sqrt{2}\sin\theta)$. Moreover, $\hat{n}=|2\rangle\langle2|$, $\hat{\mathbf{1}}=|1\rangle\langle1|+|2\rangle\langle2|$ and $\tau^+=|1\rangle\langle2|\equiv\hat{b}^\dagger$.

Since the XY model on triangular lattice exhibits chiral order [27], we also calculate it in the ground state of $\hat{H}_{\geq\frac{1}{2}}$ as a function of h. The z-component of chirality of an upright triangle at position $\mathbf{R}$ is written as, $\chi^z(\mathbf{R})=(\vec{\tau}_1\times\vec{\tau}_2)_z+(\vec{\tau}_2\times\vec{\tau}_3)_z+(\vec{\tau}_3\times\vec{\tau}_1)_z$, where 1, 2 and 3 are the spins of that triangle. The chiral order parameter is defined as: $\chi=\sqrt{[\sum_{\mathbf{R}}\chi^z(\mathbf{R})]^2/LS(LS+1)}$, where $S=1/2$ and $\mathbf{R}$ runs over the upright triangles of a cluster [27]. The data in Fig. 6 clearly indicates the presence of chiral order for M/M_{sat} between 1/2 and 1, while the plateaus are absent. Close to 1/2 and 1, however, the spikiness in χ seem to indicate some anomalies that may show up in M (possibly as jumps).

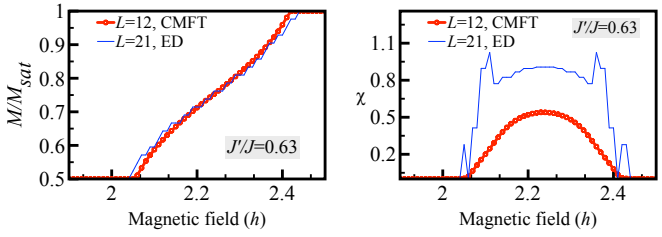

FIG. 6. Magnetisation and chirality (χ) vs. magnetic field from the exact numerical diagonalization (ED) and cluster-mean-field theory (CMFT) calculations for $M/M_{sat}\geq1/2$.

We acknowledge DST-FIST support for the computational facilities. B. D. thanks CSIR for financial support.

* bkumar@mail.jnu.ac.in

[1] B. S. Shastry and B. Sutherland, Physica B. **108**, 1069 (1981).

[2] H. Kageyama, K. Yoshimura, R. Stern, N. V. Mushnikov, K. Onizuka, M. Kato, K. Kosuge, C. P. Slichter, T. Goto, and Y. Ueda, Phys. Rev. Lett. **82**, 3168 (1999).

[3] S. Miyahara and K. Ueda, Phys. Rev. Lett. **82**, 3701 (1999).

[4] B. S. Shastry and B. Kumar, Prog. Thoer. Phys. (Suppl) **145**, 1 (2002).

[5] K. Onizuka, H. Kageyama, Y. Narumi, K. Kindo, Y. Ueda, and T. Goto, J. Phys. Soc. Jpn. **69**, 1016 (2000).

[6] S. E. Sebastian, N. Harrison, P. Sengupta, C. D. Batista, S. Francoual, E. Palm, T. Murphy, N. Marcano, H. A. Dabkowska, and B. D. Gauline, PNAS **105**, 20157 (2008).

[7] M. Takigawa, M. Horvatić, T. Waki, S. Krämer, C. Berthier, F. Lévy-Bertrand, I. Sheikin, H. Kageyama, Y. Ueda, and F. Mila, Phys. Rev. Lett. **110**, 067210 (2013).

[8] M. Jaime, R. Daou, S. A. Crooker, F. Weickert, A. Uchida, A. E. Feiguine, C. D. Batista, A. D. Hanna, and B. D. Gauling, PNAS **109**, 12404 (2012).

[9] Y. H. Matsuda, N. Abe, S. Takeyama, H. Kageyama, P. Corboz, A. Honecker, S. R. Manmana, G. R. Foltin, K. P. Schmidt, and F. Mila, Phys. Rev. Lett. **111**, 137204 (2013).

[10] S. Miyahara and K. Ueda, J. Phys.: Condens. Matter **15**, R327 (2003).

[11] The dimer-singlet state is the exact ground state of H_{SS} for $J'/J \lesssim 0.677$ [28, 29].

[12] O. Cépas, K. Kakurai, L.-P. Regnault, T. Ziman, J.-P. Boucher, N. Aso, M. Nishi, H. Kageyama, and Y. Ueda, Phys. Rev. Lett. **87**, 167205 (2001).

[13] K. Kodama, S. Miyahara, M. Takigawa, M. Horvatic, C. Berthier, F. Mila, H. Kageyama, and Y. Ueda, J. Phys.: Condens. Matter **17**, L61 (2005).

[14] J. Romhányi, K. Totsuka, and K. Penc, Phys. Rev. B **83**, 024413 (2011).

[15] T. Momoi and K. Totsuka, Phys. Rev. B **62**, 15067 (2000).

[16] K. Kodama, M. Takigawa, M. Horvatic, C. Berthier, H. Kageyama, Y. Ueda, S. Miyahara, F. Becca, and F. Mila, Science **298**, 395 (2002).

[17] M. Takigawa, S. Matsubara, M. Horvatić, C. Berthier, H. Kageyama, and Y. Ueda, Phys. Rev. Lett. **101**, 037202 (2008).

[18] J. Dorier, K. P. Schmidt, and F. Mila, Phys. Rev. Lett. **101**, 250402 (2008).

[19] A. Abendschein and S. Capponi, Phys. Rev. Lett. **101**, 227201 (2008).

[20] G. Misguich, T. Jolicoeur, and S. M. Girvin, Phys. Rev. Lett. **87**, 097203 (2001).

[21] By a dimer-hard-core boson, we mean the usual two-level object given by the singlet and a fully polarised triplet on a dimer of quantum spins [Cu^{2+} ions in $SrCu_2(BO_3)_2$]. In a magnetic field, these two dimer states come together to form a minimal dimer-subspace which is typically considered relevant to discuss the magnetisation properties of the dimerised antiferromagnets.

[22] For instance, a similar lack of faith in the standard belief that dimer-triplets crystallise to form plateaus in SS model has been expressed recently in Ref. [30].

[23] Our V'' is similar to V_3' in Refs. [18, 19], and V''' is roughly like their V_7 which is $\lesssim V_3'$. While mostly V_3' and V_7 are negligible (consistent with the absence of V'' and V''' in our minimal $\hat{H}_0$), but they begin to show up for big enough J'/J. Our heuristic estimate of V'' is numerically not badly off from the values of V_3' in these references.

[24] Bimla, *Magnetization Plateaus in Shastry-Sutherland Model, and Two Other Studies on Frustrated Quantum Spins*, Ph.D. thesis, Jawaharlal Nehru University, New Delhi (2014).

[25] By dynamic inhomogeneity of a transverse field, here we mean that it is determined dynamically by the hard-core particles' occupancies at different sites.

[26] P. Bak, Rep. Prog. Phys. **45**, 587 (1982).

[27] N. Suzuki and F. Matsubara, Phys. Rev. B **55**, 12331 (1997).

[28] A. Koga and N. Kawakami, Phys. Rev. Lett. **84**, 4461 (2000).

[29] P. Corboz and F. Mila, Phys. Rev. B **87**, 115144 (2013).

[30] P. Corboz and F. Mila, Phys. Rev. Lett. **112**, 147203 (2014).